Rotating Convection in an Anisotropic System

Alex Roxin and Hermann Riecke
Engineering Science and Applied Mathematics, Northwestern University, Evanston, Il 60208, USA
(February 8, 2008)

We study the stability of patterns arising in rotating convection in weakly anisotropic systems using a modified Swift-Hohenberg equation. The anisotropy, either an endogenous characteristic of the system or induced by external forcing, can stabilize periodic rolls in the Küppers-Lortz chaotic regime. For the particular case of rotating convection with time-modulated rotation where recently, in experiment, chiral patterns have been observed in otherwise Küppers-Lortz-unstable regimes, we show how the underlying base-flow breaks the isotropy, thereby affecting the linear growth-rate of convection rolls in such a way as to stabilize spirals and targets. Throughout we compare analytical results to numerical simulations of the Swift-Hohenberg equation.

arXiv:nlin/0110041v1 [nlin.PS] 22 Oct 2001

I. INTRODUCTION

Pattern formation in thermal convection of a rotating fluid layer has been the subject of much experimental and theoretical work in recent years. The effect of the Coriolis force on the dynamics of thermal instabilities makes this system relevant for both astrophysical and geophysical fluid dynamics, while the appearance of spatio-temporally chaotic dynamics near onset make it an attractive candidate for detailed analytical and numerical investigations of the origin and behavior of chaotic complex patterns.

Küppers and Lortz [1] determined that for rotation rates greater than a critical value $\Omega > \Omega_{cr}$ steady convective roll patterns are unstable to another set of rolls oriented at an angle β relative to the first. These results were confirmed and extended by Clever and Busse [2] who also determined the dependence of Ω_{cr} and β on the Prandtl number of the fluid. In an infinite system, these dynamics are persistent due to isotropy. Busse and Heikes [3] used this fact, and the closeness of β to $\frac{\pi}{3}$ to derive three coupled amplitude equations, in which rolls switch cyclicly as they approach a heteroclinic orbit. In real systems, small amplitude noise perturbs this orbit, leading to nearly periodic switching of rolls. In sufficiently large systems the switching becomes incoherent in space and causes the development of patches of rolls with different orientations. The ensuing dynamics are chaotic, [4], [5].

In recent experiments on rotating convection [6], Thompson, Bajaj and Ahlers investigated the effect of a temporal modulation of the rotation rate on the Küppers-Lortz (KL) state. They find that for sufficiently large modulation concentric roll patterns (targets) as well as multi-armed spirals can be stabilized and replace the chaotic KL state. Focusing on the target pattern, they find that the rolls in these patterns drift radially inward and they measure the dependence of the drift velocity on modulation amplitude and frequency, mean rotation rate, and heating. They point out, the modulation sets up an oscillatory azimuthal mean flow, which tends to align rolls along that direction. Since the alignment signles out a specific orientation, it breaks the isotropy of the system. Motivated by these findings we therefore investigate here the effect of anisotropy on roll patterns in systems exhibiting KL chaos.

Within the framework of a suitably extended SH-model we first study the stability of straight rolls in systems with broken chiral symmetry (modeling the Coriolis force due to rotation) and with weak anisotropy. We then use these analytical results to interpret simulation of this SH-model in a cylindrical geometry in which we obtain target and spiral patterns as seen in experiment.

II. THE STABILITY OF ROLLS WITH ANISOTROPY

We study the effect of weak anisotropy on the Küppers-Lortz state in the following modified Swift-Hohenberg model,

$$\partial_t \psi = \mu\psi + \alpha^2(\hat{n}\cdot\nabla)^2\psi - (\nabla^2+1)^2\psi - \psi^3 + \gamma\hat{k}\cdot[\nabla\times[(\nabla\psi)^2\nabla\psi]], \tag{1}$$

where $\hat{n}$ is a director indicating the preferred orientation, and α gives the strength of this anisotropy. We retain the up-down (Boussinesq) symmetry ($\psi \to -\psi$) by including only odd terms in ψ, and include a nonlinear gradient term that breaks the chiral symmetry. The rotation rate is therefore measured by γ. Similar models have been systematically derived from the fluid equations, with [7] and without [8,9] mean flow effects, and have enjoyed widespread use, e.g.

[10–13]. We mean (1) to be a model equation and are concerned with the *qualitative* effect of anisotropy on the Küppers-Lortz instability.

Focusing on the weakly nonlinear regime and assumimg the anisotropy to be weak, we take $\mu = \epsilon^2\mu_2$ and $\alpha = \epsilon\alpha_2$ with $\epsilon \ll 1$. To leading order in ϵ the system is therefore isotropic. To study the effect of the anisotropy on the KL-instability we consider the weakly nonlinear competition of two sets of rolls with relative angle β with the ansatz,

$$\psi = \epsilon(A(\tau)e^{i(\cos(\theta)x+\sin(\theta)y)} + B(\tau)e^{i(\cos(\theta+\beta)x+\sin(\theta+\beta)y)} + c.c.) + h.o.t. \tag{2}$$

Thus here we do not analyze all side-band instabilities. To leading order the system is isotropic and θ is a free parameter. The complex amplitudes A and B evolve on the slow timescale $\tau = \epsilon t$. For concreteness we take $\hat{n} = \hat{e}_y$. At order ϵ^3, a solvability condition yields

$$\partial_\tau A = \mu_2 A - \alpha^2 \sin^2(\theta)A - 3|A|^2A - (6 + 4\gamma \sin\beta\cos\beta)|B|^2A, \tag{3}$$
$$\partial_\tau B = \mu_2 B - \alpha^2 \sin^2(\theta+\beta)B - 3|B|^2B - (6 - 4\gamma \sin\beta\cos\beta)|A|^2B. \tag{4}$$

We examine the stability of rolls of orientation θ with respect to a set of rolls oriented β to the first set of rolls. With $\alpha = 0$ (isotropic case), the absolute orientation of the rolls θ is irrelevant, and we find they become first unstable to rolls with orientation

$$\beta_{KL} = 45^o \tag{5}$$

for

$$\gamma \geq \gamma_{KL} = \frac{3}{2}. \tag{6}$$

Introducing $\alpha \neq 0$ leads to a dependence of both β_{KL} and γ_{KL} on the obsolute orientation of the rolls θ. The growth rates of the perturbations are given by

$$\sigma_A = -2(\mu_2 - \alpha^2 \sin^2\theta), \tag{7}$$
$$\sigma_B = \mu_2(-1 + \frac{4}{3}\gamma \sin\beta\cos\beta) - \alpha(\sin^2\theta + \beta + [\frac{4}{3}\gamma \sin\beta\cos\beta - 2]\sin^2\theta). \tag{8}$$

As can be seen from (7) the anisotropy has shifted the onset of rolls with orientation θ to

$$\mu_2(\hat{\theta}) = \alpha_2^2 \sin^2\hat{\theta}. \tag{9}$$

Thus rolls with orientation θ exist for $\mu_2 > \mu_{2cr}(\theta)$. For fixed μ this implies a neutral curve $\alpha(\theta)$ as shown by the dashed line in Figure 1. Rolls of orientation θ first become unstable to rolls of different orientation at

$$\sigma_B \quad = \quad \frac{\partial\sigma_B}{\partial\beta} = 0. \tag{10}$$

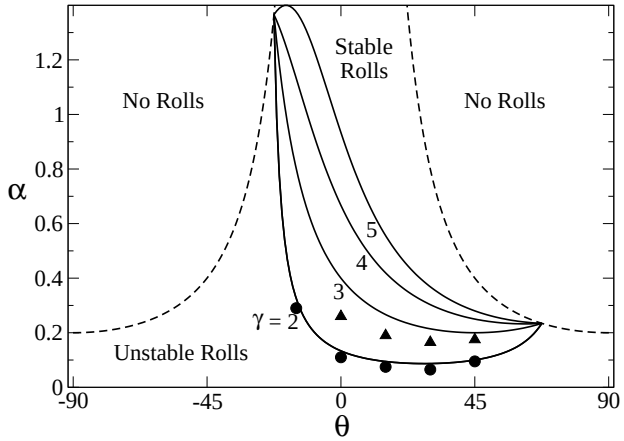

FIG. 1. Linear stability diagram of rolls with orientation θ in (3, 4) with respect to rolls at a relative orientation of β_{KL}. Here $\mu = 0.2$. Numerical results are given by the solid symbols: triangles for $\gamma = 3$ and circles for $\gamma = 2$.

Equation (10) must be solved numerically for the linear stability limits. Results are given in Figure 1 for various values of γ (solid lines). To test these stability results we perform numerical simulations in which we perturb straight rolls of orientation θ by small-amplitude rolls of orientation $\theta + \beta$, where β is chosen as the angle corresponding to the maximal growth rate according to (10). To verify that no additional instabilities are present, we also perturb the rolls with small-amplitude noise. As can be seen from the solid symbols in Figure 1, numerical simulations agree well with the weakly nonlinear analysis for rotation rates γ that are not too far above $\gamma_{KL}(\alpha) \sim 1.5$, for which only weak anisotropy is needed for stability. For larger rotations rates γ, the weakly nonlinear theory overestimates the amount of anisotropy α needed to stabilize rolls. For $\alpha = O(1)$ the anisotropy affects the linear growth rate of rolls already in (1) and will introduce a significant dependence of the critical wavenumber on the orientation θ. Numerical results for larger α reveal that large amplitude rolls (with $\theta = 0$) tend to grow and invade regions of rolls of other orientations front-wise. In fact, for $\alpha \to \infty$ only rolls with $\theta = 0$ exist.

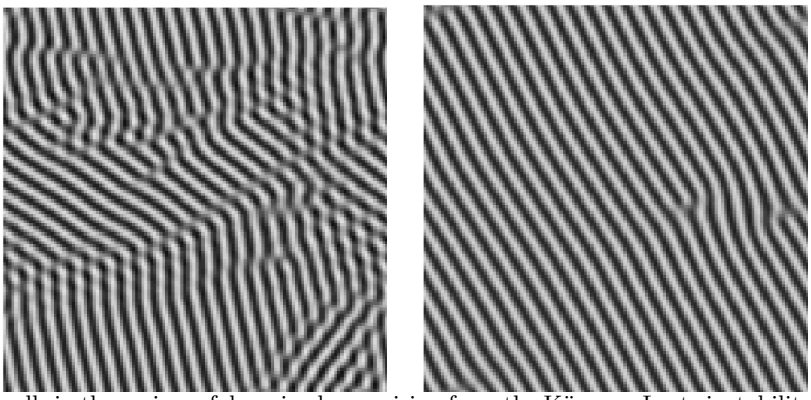

FIG. 2. Stabilization of rolls in the regime of domain chaos arising from the Küppers-Lortz instability. a) A typical patch-work pattern of domain chaos, where the angle between patches $\beta_{KL} = 45$, and $\gamma = 2.0, \mu = 0.2, \alpha = 0.0$). b) For the same values of the parameters with $\alpha^2 = 0.15$, rolls are stabilized.

Thus, weak anisotropy can stabilize periodic rolls arising in rotating convection in the Küppers-Lortz unstable regime. Specifically, there is a finite band of angles θ with respect to the anisotropic director $\hat{n}$ such that rolls with this angle are stable to homogenous perturbations of all possible orientations.

III. MODULATED ROTATING CONVECTION: SPIRALS AND TARGETS

We now turn to the specific problem of rotating convection with periodically modulated rotation. A thin layer of fluid of height d is heated from below and bounded above and below by a rigid plate, which is rotated with an angular velocity $\Omega = \Omega_o(1 + \delta \cos \omega t)$. For $\delta = 0$ we recover the well-studied case of rotating convection [1]- [7], [10,11,14]. For $\delta \ll 1$ but nonzero, a nontrivial base flow is induced by the periodic motion of the rigid plates. This flow advects perturbations leading to thermal instabilities in such a way as to affect their growth rate. Indeed, far from the axis of rotation, the onset of the thermal instability is dependent on the orientation of periodic-roll perturbations with respect to the base flow in a manner analogous to the linear operator in (1), [15]. Closer to the axis of rotation, the curvature of the base flow becomes significant and a straight-roll approximation is not a good one.

The dynamics are given by the Boussinesq fluid equations in a frame rotating at the mean angular velocity Ω_0 [1]-[5] with rigid boundary conditions, which require the azimuthal velocity component at the top and bottom plates to obey,

$$u_\theta = \Re(\delta \Omega_0 r e^{i\omega t}). \tag{11}$$

This condition induces an azimuthal shear flow, the strength of which grows with distance from the axis of rotation. If we assume our flow is restricted to a finite geometry, Coriolis forces acting on this flow can be balanced by the radial pressure gradient as with the centrifugal force.

Far from the axis of rotation and, w.l.o.g., along the x-axis, the non-dimensionalized flow takes the form,

$$u_\theta = \delta \Re \left(Pr\, \tau x \frac{\sinh kz - \sinh k(z-1)}{2 \sinh k} e^{iPr\, \omega t} \right), \tag{12}$$

where the plates are located at $z = 0, 1$, $k = \sqrt{\frac{\omega}{2}}(1 + i)$ and

$$Pr = \frac{\nu}{\kappa}, \qquad \tau = \frac{2\Omega_0 d^2}{\nu}, \tag{13}$$

where the modulation frequency ω has been nondimensionalized with respect to the viscous diffusion time. Note that (12) satifies the equation of continuity, $\nabla \cdot \mathbf{u} = \mathbf{0}$.

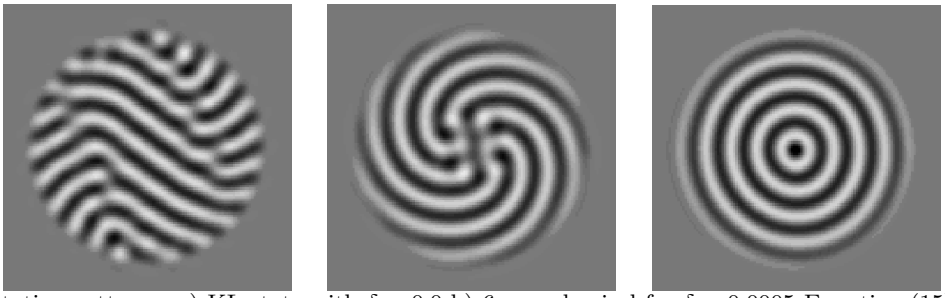

FIG. 3. Representative patterns: a) KL-state with $\delta = 0.0$ b) 6-armed spiral for $\delta = 0.0005$ Equation (15) predicts six arms in this case. c) Target pattern for $\delta = 0.001$. For all three $\gamma = 2.0$, $\mu = 0.2$ and the system size $L = 72$.

Thermal instabilities arising from the imposed temperature gradient are advected by (12) and hence parametrically forced with frequency $Pr\omega$. Rayleigh-Bénard convection has been studied with time-modulated heating [16–19], and time-modulated gravity (parametrically accelerated) [20]. Here we note the following two facts which will allow us to deduce the effect of the base-flow (12) on the instabilities to leading order. Firstly, near onset, the dynamics of the instability are slow compared with the period of the oscillatory shear-flow for any finite rotation rate. Secondly, the forcing is invariant under the transformation $\delta \to -\delta, t \to t + \frac{\pi}{Pr\omega}$. Averaging over the fast oscillations with respect to the slow dynamics near onset, the base-flow affects the growth-rate of thermal instabilities through mean-squared contributions (proportional to δ^2). For the case (12), the correction to the growth rate is of the form $u_\theta^2 \partial_y^2$, whereas consideration of the full, cylindrical geometry yields $\frac{1}{r^2} u_\theta(r)^2 \partial_\theta^2$.

With the abovementioned assumptions, we study the dynamics of patterns in (1) with,

$$\alpha^2 = \delta^2 r^2, \qquad \hat{n} = \hat{e}_\theta. \tag{14}$$

We note that the scaling of the anisotropy (14) as linear in the distance from the axis of rotation, is only correct far from the axis itself. However, we retain this simplified form and hope to extract qualitatively correct results. In fact, simulations with other polynomial dependencies have revealed that only the monotonicity of the function is important in determining qualitative features of the patterns.

Simulations reveal a wide variety of spiral patterns as well as targets. For small δ, where we expect the weakly-nonlinear theory for periodic rolls to be valid sufficiently far from the core of the spiral, we are able to predict the number of spiral-arms with reasonable accuracy. Such an analysis can be understood from Figure 1. For a fixed 'rotation-rate' γ, the strength of anisotropy α increases with distance from the core of the spiral. There is thus a region in the vicinity of the core where no rolls are stable, and rolls of a given orientation θ^* are selected at a distance r^* as determined by condition (10). The number of resulting spiral-arms is then given by geometry as,

$$N = q r^* \sin\theta^*, \tag{15}$$

where q is the wavenumber of the rolls (arms).

Spirals or targets can be generated for the same parameter values given different initial conditions. In general an initial straight roll pattern will result in a target for sufficiently large δ whereas disordered initial conditions generically yield spirals, even for strong anisotropy.

Interestingly, the orientation-selection mechanism given by (15) predicts the possibility of a large region surrounding the core, within which no rolls are stable in the context of the weakly nonlinear theory. If the anisotropy is sufficiently weak, one should see a disordered region of domain chaos, bounded by a stable spiral, given a large enough system. Such a pattern is shown in Figure 4.

IV. CONCLUSION

Spirals and targets arising in Rayleigh-Bénard convection have been the subject of much theory and experimental work, [7,4,11,21–23]. Target patterns in low-Prandtl number convection are a consequence of horizontal, thermal

gradients at the sidewalls of a cylindrical container, which tend to align rolls parallel to the walls [23]. Even with sidewall forcing, the targets become unstable to straight rolls relatively close to threshold. In rotating convection, the target patterns arising from such sidewall forcing undergo a mean drift [11] due to the breaking of reflection symmetry by the applied rotation. However, in the case of rotating convection with a modulated rotation rate, the chiral patterns are not a consequence of the system geometry, but rather are induced by an isotropy-breaking shear flow, which acts azimuthally. We have shown that these patterns are stable in regimes where one would see spatio-temporal chaos in the absence of modulation. Our analysis indicates that the shear flow acts to stabilize rolls within a band of stable orientations w.r.t. the azimuthal flow itself. This leads naturally to a chiral pattern.

The qualitative agreement between the types of patterns observed in experiment [6] and those studied here make the selection mechanism described in section III plausible. Spirals and targets arise through the interaction of the destabilizing process responsible for the KL instability and the stabilizing effect of the azimuthal mean flow (MF). Quantitative comparison of the dependence of the pattern behavior on the reduced Rayleigh number, rotation rate, and amplitude and frequency of the modulation with experiment is, however, not possible within the framework of (1). However, qualitatively the genericity of the appearance of spirals patterns under modulated rotation with disordered intial conditions (KL state) seems to hold both under experimental conditions and here. Targets, on the other hand, must be generated with care but then persist as stable patterns over a wide range of parameter values.

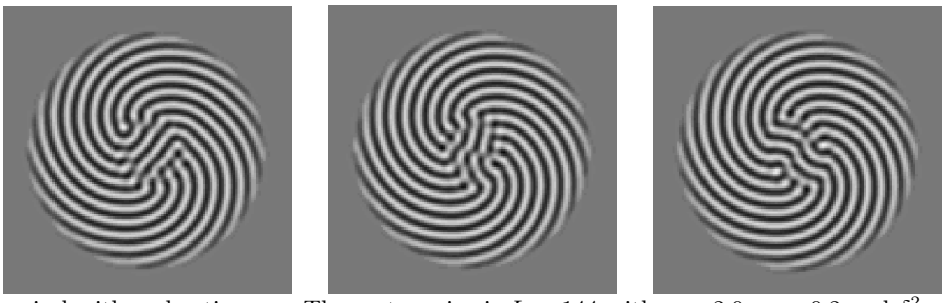

FIG. 4. A stable spiral with a chaotic core. The system size is $L = 144$ with $\gamma = 2.0$, $\mu = 0.2$ and $\delta^2 = 0.0001$. Note that equation (15) predicts 14 arms. The core dynamics occur on a fast timescale w.r.t. the slow, solid-body rotation of the outer spiral.

The target patterns observed in [6] travel inwards radially, collapsing periodically at the center. The origin of this drift has not been identified yet. One possibility is that the time-periodic component of the Coriolis force acting on the time-periodic azimuthal flow generates a radial flow with a steady component, which would advect the axisymmetric roll pattern [24,25]. Another possibility is that the drift is due to a mismatch between the wavenumber selected by the umbilicus [26] and that selected by the container side-wall [27,28]. The competing selected wavenumbers set up a wavenumber gradient that induces a drift of the pattern [29,30]. It should be possible to distinguish between these two mechanisms by comparing the dynamics in systems of different aspect ratio. For larger systems, the wavenumber gradient induced by the incompatibility of the selected wavenumbers would be weakened, while the effective strength of the radial flow would naturally be stronger due to the greater Coriolis force at larger radii. Experiments in such larger systems would also be of interest in view of the prediction that in such systems the core of the spirals would exhibit chaotic dynamics of the Küppers-Lortz type.

In our simulations of (1) no radial drift of the concentric rolls was found. This is not unexpected since in the absence of the chiral-symmetry breaking term proportional to γ eq.(1) is variational and persistent dynamics are ruled out. To obtain drift the variational character of the system has to be broken to a sufficient degree. This may require much larger rotation rates γ or the introduction of additional non-variational terms. We have not pursued this further since simulations of extensions of (1) with possibly also modified boundary conditions would not allow any quantitative comparison with experiments and would therefore be of limited use in identifying the dominant mechanism responsible for the drift.

We wish to acknowledge helpful discussions with Guenter Ahlers, Vadim Moroz, and Werner Pesch. This work was supported by the Engineering Research Program of the Office of Basic Energy Sciences at the Department of Energy (DE-FG02-92ER14303), by a grant from NSF (DMS-9804673), and by a NSF-IGERT fellowship through grant DGE-9987577.

[1] G. Küppers and D. Lortz, J. Fluid Mech. **35**, 609 (1969).
[2] R. Clever and F. Busse, J. Fluid Mech. **94**, 609 (1979).
[3] F. Busse and K. Heikes, Science **208**, 173 (1980).
[4] Y. Hu, R. Ecke, and G. Ahlers, Phys. Rev. E **55**, 6928 (1997).
[5] Y. Hu, W. Pesch, G. Ahlers, and R. E. Ecke, Phys. Rev. E **58**, 5821 (1998).
[6] K. L. Thompson, K. M. Bajaj, and G. Ahlers, Phys. Rev. E (submitted).
[7] Y. Ponty, T. Passot, and P. Sulem, Phys. Fluids **9**, 67 (1997).
[8] M. Neufeld, R. Friedrich, and H. Haken, Z. Phys. B **92**, 243 (1993).
[9] A. Mancho, H. Riecke, and F. Sain, preprint .
[10] J. Millán-Rodríguez *et al.*, Phys. Rev. A **46**, 4729 (1992).
[11] M. Fantz, R. Friedrich, M. Bestehorn, and H. Haken, Physica D **61**, 147 (1992).
[12] F. Sain and H. Riecke, Physica D **144**, 124 (2000).
[13] M. Cross, D. Meiron, and Y. Tu, Chaos **4**, 607 (1994).
[14] R. Worthing, Phys. Lett. **237**, 381 (1998).
[15] R. E. Kelly, in *Physiochemical Hydrodynamics*, edited by D. B. Spalding (1987), p. 65.
[16] M. N. Roppo, S. H. Davis, and S. Rosenblat, Phys. Fluids **27**, 796 (1984).
[17] P. C. Hohenberg and J. B. Swift, Phys. Rev. A **35**, 3855 (1987).
[18] J. J. Niemela and R. J. Donnelly, Phys. Rev. Lett. **59**, 2431 (1987).
[19] C. Meyer *et al.*, Phys. Rev. Lett. **61**, 947 (1988).
[20] P. M. Gresho and R. L. Sani, J. Fluid Mech. **40 part 4**, 783 (1970).
[21] Y. Hu, R. Ecke, and G. Ahlers, Phys. Rev. Lett. **72**, 2191 (1994).
[22] R. Ecke, Y. Hu, R. Mainieri, and G. Ahlers, Science **269**, 1704 (1995).
[23] Y. Hu, R. Ecke, and G. Ahlers, Phys. Rev. E **48**, 4399 (1993).
[24] W. Pesch, priv. comm. .
[25] V. Moroz, priv. comm. .
[26] Y. Pomeau and P. Manneville, J. Phys. (Paris) **42**, 1067 (1981).
[27] M. C. Cross, P. G. Daniels, P. C. Hohenberg, and E. D. Siggia, J.Fluid Mech. **127**, 155 (1983).
[28] P. Hohenberg, L. Kramer, and H. Riecke, Physica D **15**, 402 (1985).
[29] L. Kramer, E. Ben-Jacob, H. Brand, and M. Cross, Phys. Rev. Lett. **49**, 1891 (1982).
[30] H.-G. Paap and H. Riecke, Phys. Fluids A **3**, 1519 (1991).